

# Gas-Phase Generation and Electronic Structure Investigation of Oxidovanadium Triisocyanate, $\text{OV}(\text{NCO})_3$

Maofa Ge,<sup>\*[a]</sup> Weigang Wang,<sup>[a,b]</sup> Shi Yin,<sup>[a,b]</sup> and Carlos O. Della Védova<sup>[c]</sup>

**Keywords:** Vanadium / Photoelectron spectroscopy / Electronic structure / Mass spectrum

Oxidovanadium triisocyanate was generated from the heterogeneous reaction of gaseous vanadium trichloride oxide with silver cyanate and studied for the first time in the gas phase. The reaction processes were studied in situ by ultraviolet photoionization mass spectrometry combined with

quantum chemical calculations and ultraviolet photoelectron spectrometry. The geometric and electronic structures were characterized and discussed.

(© Wiley-VCH Verlag GmbH & Co. KGaA, 69451 Weinheim, Germany, 2008)

## Introduction

High-valent transition-metal oxo compounds, including  $\text{OVCl}_3$ , are often used as potent yet selective oxidizing agents in organic synthesis.<sup>[1]</sup> There are many studies on transition-metal oxides in the gas phase, because of their application in catalysis and materials chemistry.<sup>[2]</sup> The oxides of vanadium are prevalently used in industrial heterogeneous catalysis,<sup>[3]</sup> which involves oxidation of hydrocarbons to anhydrides,  $\text{SO}_2$  to  $\text{SO}_3$ , and other reactions. Vanadium complexes containing N-, O-donor ligands are of considerable interest, because such complexes have been used as insulin mimetics and are potential therapeutic agents for diabetes mellitus.<sup>[4]</sup>

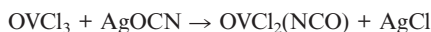
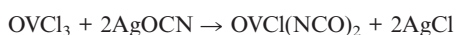
Isocyanates are esters of isocyanic acid, which are important in the formation of polyurethanes that offer interesting possibilities for a variety of important applications.<sup>[5,6]</sup> The substitution on an isocyanate, thiocyanate, or azide group leads to interesting spectroscopic properties caused by the splitting of the  $\pi$  degeneracy. Relative to numerous studies on vanadium compounds in the solid state, there is only little research about vanadium-containing compounds in the gas phase.  $\text{OV}(\text{NO}_3)_3$  was first found by M. Schmeisser 40 years ago,<sup>[7]</sup> while the structure was fixed a few years ago.<sup>[8]</sup> Schröder et al. have investigated the ion chemistry of  $\text{OV}(\text{OCH}_3)_3$  to explain the mechanisms of oxidation reactions catalyzed by transition-metal oxides.<sup>[9]</sup>

We have a long-standing interest in the generation, spectroscopy, and electronic structure of unstable species in the gas phase.<sup>[10–12]</sup> Herein we present the first in situ generation of oxidovanadium triisocyanate in the gas phase and its subsequent characterization by photoelectron spectroscopy (PES) and photoionization mass spectrometry (PIMS). The experimental ionization energies have been assigned with the aid of Outer-Valence Green's Function (OVGF) calculations. Three-dimensional MO plots were obtained with the GaussView program. Each orbital is displayed with the 0.06 isodensity value and is oriented in a way that provides the best view.

## Results and Discussion

### Photoionization Mass Spectrometry

The reaction process for generating oxidovanadium triisocyanate was monitored by PIMS. The mass spectra of the reaction products of  $\text{VOCl}_3$  and  $\text{AgOCN}$  at different temperatures are shown in Figure 1. The spectrum of the reaction mixture at room temperature shows the typical isotope and fragmentation pattern of  $\text{OVCl}_3$ .<sup>[13]</sup> It was demonstrated that the reaction was very slow at room temperature. As the temperature was increased to 40 °C, the peaks of  $\text{OVCl}_3$  became weak and other peaks appeared in the spectrum. There were two series of peaks in the mass spectrum in addition to the peaks belonging to the reactant. The appearance of the  $\text{OV}(\text{NCO})\text{Cl}_2$  molecular ion confirmed the generation of  $\text{OV}(\text{NCO})\text{Cl}_2$ . The appearance of  $\text{OV}(\text{NCO})_2^+$  and the parent ion  $[\text{OV}(\text{NCO})_2\text{Cl}]^+$  confirmed the generation of  $\text{OV}(\text{NCO})_2\text{Cl}$ . Although we tried to control the temperature of the reaction more precisely, we could not separate the compounds mentioned above from each other. The following reactions are possible:



[a] State Key Laboratory for Structural Chemistry of Unstable and Stable Species, Beijing National Laboratory for Molecular Sciences (BNLMS), Institute of Chemistry, Chinese Academy of Sciences,

100080 Beijing, P. R. China

Fax: +86-10-62554518

E-mail: gemaofa@iccas.ac.cn

[b] Graduate University of the Chinese Academy of Sciences, 100039 Beijing, P. R. China

[c] CEQUINOR (CONICET-UNLP), Departamento de Química, Facultad de Ciencias Exactas, Universidad Nacional de La Plata, C. C. 962 (1900) La Plata, República Argentina

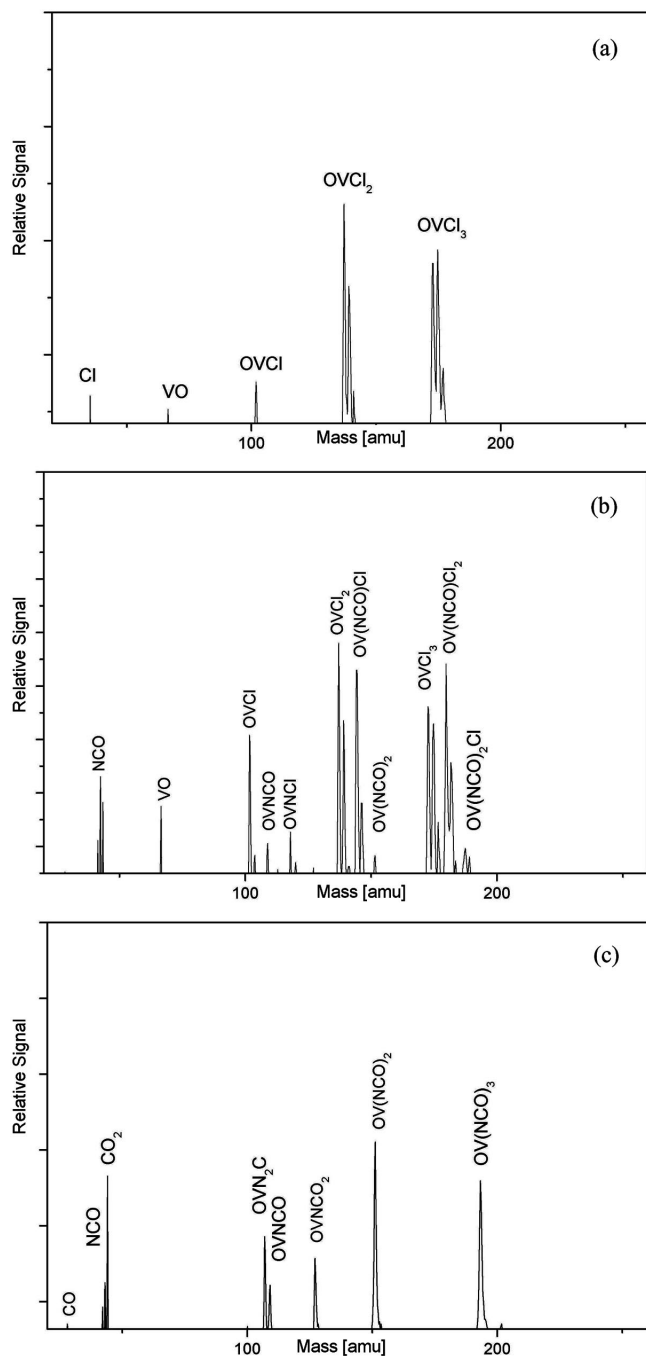


Figure 1. Photoionization mass spectra of  $\text{OVCl}_3$  (a), the gaseous products of the reaction at 40 °C (b), and the gaseous products of the reaction at 130 °C (c).

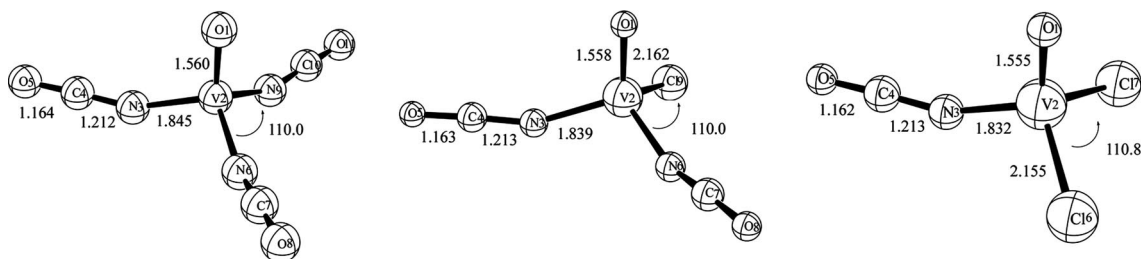


Figure 2. Geometry for  $\text{OV}(\text{NCO})_3$ ,  $\text{OVCl}(\text{NCO})_2$ , and  $\text{OVCl}_2(\text{NCO})$  at the B3LYP/6-311++G(d,p) level of theory.

Figure 1c illustrates the photoionization mass spectrum of the gaseous products of the reaction at 130 °C, which is distinct from Figure 2b. The mass spectrum is relatively simple: there are peaks at  $m/z = 42$ , 44, 107, 109, 151, and 193. The parent ion is assigned to be  $m/z = 193$  [ $\text{OV}(\text{NCO})_3$ ], and the peak at  $m/z = 151$  represents a loss of 42 amu (NCO).

By analyzing these results, we deduced the process of the reaction. The substitution is incomplete at low temperature. When the temperature is higher than 130 °C, the complete substitution product can be obtained as the only product in the gas phase.

## Molecular Structure

There is much experimental and theoretical research focused on novel species composed of vanadium, nitrogen, and oxygen in the solid phase,<sup>[14]</sup> but few examples of compounds containing the V–N bond have been observed in the gas phase. Theoretical calculations have been used to provide information on structures and relative energies. Geometry optimization was performed for  $\text{OV}(\text{NCO})_3$ ,  $\text{OVCl}(\text{NCO})_2$ , and  $\text{OVCl}_2(\text{NCO})$  by using the DFT method. The structural parameters are depicted in Figure 2.  $\text{OV}(\text{NCO})_3$ ,  $\text{OVCl}(\text{NCO})_2$ , and  $\text{OVCl}_2(\text{NCO})$  possess  $C_{3v}$ ,  $C_s$ , and  $C_s$  symmetry, respectively. Comparing the V=O bond of several compounds, we found that the predicted V=O bond length in  $\text{OV}(\text{NCO})_3$  (1.560 Å) is very close to the experimental results for  $\text{OV}(\text{NO})_3$  (1.607 Å) and  $\text{OVCl}_3$  (1.571 Å) in the gas phase.<sup>[8,15]</sup> The V=O bonds in  $\text{OVCl}(\text{NCO})_2$  and  $\text{OVCl}_2(\text{NCO})$  are slightly shorter than that in  $\text{OV}(\text{NCO})_3$ . The V–N bond of  $\text{OV}(\text{NCO})_3$  (1.845 Å) is close to the value for  $\text{OV}(\text{NH}_2)_3$  (1.866 Å) predicted by calculation,<sup>[16]</sup> the V–N bond becomes stronger with increasing Cl substitution, which is reflected in the decrease of  $r_{\text{V-N}}$  from 1.845 to 1.832 Å (Figure 2). An analogous phenomenon was observed in the  $\text{B}(\text{NCO})_{3-x}\text{Cl}_x$  system.<sup>[17]</sup> The calculated angle N–C–O is 177.3°, which is very close to that of  $\text{SiH}_3\text{NCO}$  (180.0°).<sup>[18]</sup>

## Photoelectron Spectroscopy

The HeI photoelectron spectrum of  $\text{OV}(\text{NCO})_3$  is shown in Figure 3. Table 1 lists experimental vertical ionization energies (IE in eV), theoretical vertical ionization energies ( $E_v$

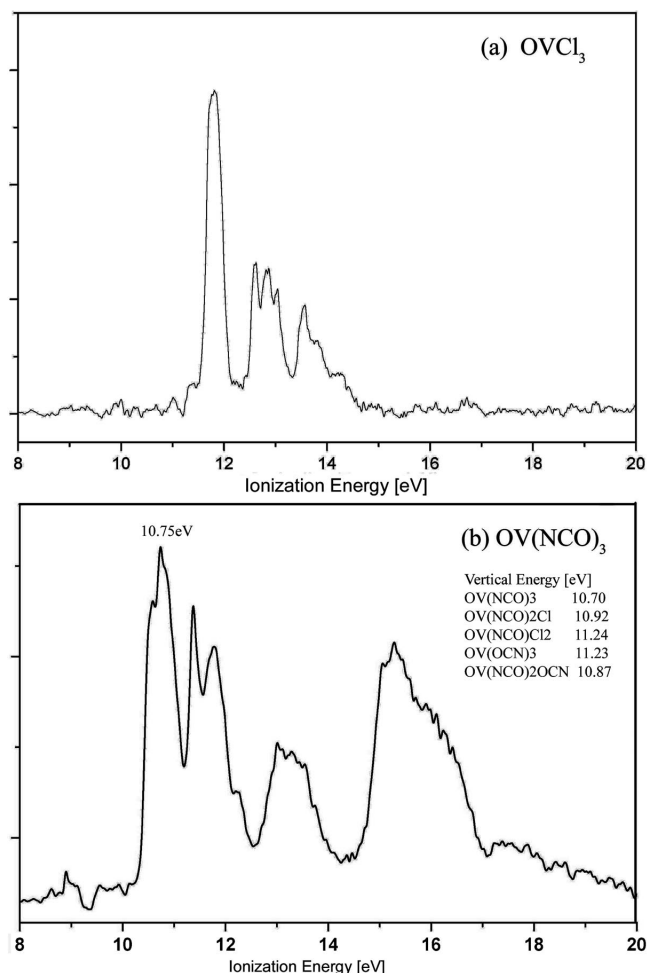


Figure 3. HeI photoelectron spectrum of  $\text{OVCl}_3$  (a) and  $\text{OV}(\text{NCO})_3$  (b).

in eV), molecular orbital symmetries, and characters of outer valence shells for  $\text{OV}(\text{NCO})_3$  calculated by OVGF. The calculated results for  $\text{OVCl}(\text{NCO})_2$  and  $\text{OVCl}_2(\text{NCO})$  are also presented in Table 1. The first vertical ionization energy ( $E_v$  in eV) was obtained from the total energy difference between the resulting cationic and neutral species in this study for comparison with the results of the OVGF calculation (Table 1). The existence of the reactants prevented the detection of products of incomplete substitution by PES. Fortunately, when the temperature was higher than 130 °C, only products of complete substitution could be detected in the gas phase, which was proved by the results of both PES and PIMS. The calculated results have been presented in Table 1 and Figure 3. It can be seen clearly that the calculated results match relatively well the experimental ionization energies for  $\text{OV}(\text{NCO})_3$ . We only discussed the product of complete substitution,  $\text{OV}(\text{NCO})_3$ , for simplicity. Most organic isocyanates are much more stable than organic cyanates. In addition, stable isocyanates, in which the isocyanate group is attached to elements other than carbon, have been synthesized extensively, as they are important chemical intermediates.<sup>[1]</sup>

In comparison with the photoelectron (PE) spectrum of  $\text{OVCl}_3$ ,<sup>[15]</sup> the spectrum of  $\text{OV}(\text{NCO})_3$  is much more complicated, because of the participation of the NCO group. In the low ionization region (<15 eV), there are four bands with no obvious vibrational structure.

The first experimental PES peak centered at 10.75 eV matches well with the recalculated value 10.70 eV, which was obtained from the total energy difference between the resulting cationic and neutral species. However, the experimental IE value does not really match very well the value calculated by OVGF (11.19 eV, see Table 1). The experimental vertical ionization energy for the second band centered

Table 1. PES vertical ionization energies (IE in eV), vertical ionization energies ( $E_v$  in eV) computed with OVGF by using 6-31G\* basis sets, and molecular orbital characters for  $\text{OV}(\text{NCO})_3$ ,  $\text{OVCl}(\text{NCO})_2$ ,  $\text{OVCl}_2(\text{NCO})$ ,  $\text{OV}(\text{OCN})_3$ ,  $\text{OV}(\text{NCO})_2\text{OCN}$ , and  $\text{OVCl}_3$ .

Experimental <sup>[b]</sup> IE [eV]	MO	Character	Calculated <sup>[a]</sup> $E_v$ [eV]				
			$\text{OV}(\text{NCO})_3$	$\text{OV}(\text{NCO})_2\text{Cl}$	$\text{OVNCOCl}_2$	$\text{OV}(\text{OCN})_3$	$\text{OV}(\text{NCO})_2(\text{OCN})$
10.75	28a <sub>2</sub>	$\pi_{\text{nb}}$ (N3–C4–O5), $\pi_{\text{nb}}$ (N6–C7–O8), $\pi_{\text{nb}}$ (N9–C10–O11)	11.19	11.24	11.46	12.27	11.54
11.32	27e	$\pi_{\text{nb}}$ (N3–C4–O5), $\pi_{\text{nb}}$ (N6–C7–O8), $\pi_{\text{nb}}$ (N9–C10–O11)	11.46	11.49	11.75	12.51	
	26e			11.51	11.66		11.78
11.82	25a <sub>1</sub>	$\pi$ (V–N)	12.08	12.18	12.47	12.78	11.88
13.01	24e	nO1, nN3, nN6, nN9	12.79	12.69	12.84	13.27	12.37
	23e			13.03	13.25		12.68
15.11	22e	$\pi$ (V2–O1)	14.84	14.07	14.51	14.06	13.26
	21e	$\pi$ (N3–C4–O5), $\pi$ (N6–C7–O8), $\pi$ (N9–C10–O11)		15.23	14.16		13.27
15.87	20a <sub>1</sub>	$\pi$ (N3–C4–O5), $\pi$ (N6–C7–O8), $\pi$ (N9–C10–O11)	15.8	15.58	15.62	14.06	15.34
Vertical energy [eV] <sup>[c]</sup>			10.70	10.92	11.24	11.23	10.87

[a] ROVGF/6-31G\*. [b] Vertical ionization energies. [c] The first vertical ionization energy ( $E_v$  in eV) obtained from the total energy difference between the resulting cationic and neutral species.

at 11.32 eV, in good agreement with the calculated 11.46 eV, is designated as the energy of ionization of the electrons of the degenerate second highest occupied molecular orbitals (SHOMOs), orbitals 27e and 26e. The first two bands are assigned to the removal of the electron from the HOMO ( $28a_1$ ) and the SHOMO (Figure 4), which are characterized by the nonbonding  $\pi_{\text{nb}}(\text{N3}-\text{C4}-\text{O5})$ ,  $\pi_{\text{nb}}(\text{N6}-\text{C7}-\text{O8})$ , and  $\pi_{\text{nb}}(\text{N9}-\text{C10}-\text{O11})$  orbitals. The most recent experimental adiabatic ionization energy for the NCO radical was determined to be  $11.759 \pm 0.006$  eV by using PIMS;<sup>[19]</sup> the computed vertical IE at the MRSD-CI level is 11.67 eV,<sup>[20]</sup> which is very close to the value observed for  $\text{OV}(\text{NCO})_3$ . Along with the substitution of Cl by NCO, the relatively sharp bands are replaced by broader bands in the PE spectrum of  $\text{B}(\text{NCO})_{3-x}\text{Cl}_x$ .<sup>[17]</sup> An analogous phenomenon was also observed in our system. With increasing temperature, the relatively sharp bands due to Cl 3p orbitals are replaced by broader bands corresponding to NCO  $\pi$  nonbonding orbitals.

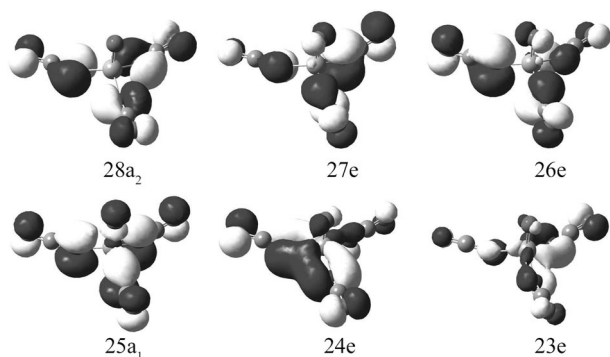


Figure 4. Characters of the first six highest occupied molecular orbitals for  $\text{OV}(\text{NCO})_3$ .

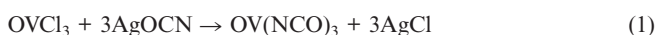
The third observed band with a vertical ionization of 11.82 eV agrees well with the calculated value 12.08 eV for orbital  $25a_1$ , as shown in Figure 4. It has  $\pi(\text{V}-\text{N})$  character. The fourth band, with an experimental vertical ionization energy of 13.01 eV, corresponding to the calculated 12.76 eV for MO 24e and 23e, has N lone-pair character. This band is also attributed to the  $\pi(\text{V}-\text{N})$  orbital formed by the interaction of V with the N lone pair (Figure 4). There are two additional bands at ionization energies higher than 15.0 eV, which are similar to those of other NCO-containing molecules. Assigning these bands is difficult, since the  $\pi$  bonds and the  $\sigma$  orbitals are predicted to lie close in energy, and most ionizations in this region ( $> 15.0$  eV) might be attributed to inner molecular orbitals with broad bands. The bands with ionization energy centered at 15.80 eV, have the magnitude (and direction) of the separation of the  $\pi(\text{NCO})$  bonding orbital (to give a and e levels), which is degenerate in the unperturbed molecule HNCO, because of the perturbations from two other NCO groups on this orbital. The last observable band below 17.0 eV is due to the ionization from the  $13a_1$ ,  $12e$ , and  $11e$  orbitals superimposed at about 17.80 eV; the primary MO character is the  $\sigma(\text{V}-\text{N})$ ,  $\sigma(\text{N}-\text{C})$ , and  $\sigma(\text{C}-\text{O})$ .

## Conclusion

In this work we have successfully generated  $\text{OV}(\text{NCO})_3$  in the gas phase for spectroscopic observation. The electronic structure of the novel molecule is characterized by in situ PES and PIMS, combined with DFT calculations. With the additional aid of the HeI photoionization mass spectrum, we investigated and deduced the possible path of the reaction between  $\text{OVCl}_3$  and  $\text{AgOCN}$ .

## Experimental Section

**Generation:**  $\text{OV}(\text{NCO})_3$  was generated by passing  $\text{OVCl}_3$  vapor over finely powdered  $\text{AgOCN}$  at 130 °C; the in situ photoelectron spectrum and mass spectrum were recorded simultaneously. The reaction may be represented by Equation (1).



The precursor  $\text{OVCl}_3$  was purchased from Alfa Company and  $\text{AgOCN}$  was purchased from ACROS Company, and their purity was better than 99%. Before reaction, silver cyanate was dried in vacuo ( $10^{-4}$  Torr) for 2 h at 60 °C.

**Instruments:** The PE spectrum was recorded with a double-chamber UPS-II machine, which was built specifically to detect transient species at a resolution of about 30 meV, as indicated by the  $\text{Ar}^+$  ( $^2\text{P}_{2/3}$ ) photoelectron band. Experimental vertical ionization energies (IE in eV) were calibrated by simultaneous addition of a small amount of argon and methyl iodide to the sample. Mass spectrometric analysis of ions is achieved with a time-of-flight mass analyzer mounted directly to the photoionization point.<sup>[21]</sup> The current mass resolution is 200. Ionization is provided by single-wavelength HeI radiation. The PE and PIMS spectra, although not acquired simultaneously, could be recorded within seconds of each other under identical conditions; thus, it is assumed that, for a given PE spectrum, the subsequent PIMS belongs to the same compound.

**Computation:** Electronic structure calculations were carried out by using the Gaussian series of programs.<sup>[22]</sup> The geometries of the molecules (both neutral ones and ions) were optimized at the B3LYP/6-311++G(d,p) levels of theory. The B3LYP is a hybrid functional method based on Becke's three-parameter nonlocal exchange functional,<sup>[23]</sup> with the nonlocal correlation of Lee, Yang, and Parr.<sup>[24]</sup> Harmonic vibrational frequencies were calculated at the same level to check whether the structure obtained is a stationary point or a saddle point. To assign the PE spectrum, Outer-Valence Green's Function (OVGF)<sup>[25]</sup> calculations were performed with the 6-31G\* basis set and on the basis of the Koopmans theorem.<sup>[26]</sup> Three-dimensional MO plots were obtained with the GaussView program. Each orbital, displayed with the 0.04 isodensity value, was oriented in a way that provided the best view.

## Acknowledgments

This project was supported by the 973 program of the Ministry of Science and Technology of China (No. 2006CB403701), the Knowledge Innovation Program (Grant No. KZCX2-YW-205), the Hundred Talents Fund of the Chinese Academy of Sciences, and the National Natural Science Foundation of China (Contract No. 20577052, 20673123).

- [1] a) S. Patai, *The Chemistry of Cyanates and Their Thio Derivatives*, Wiley, New York, 1977; b) P. Burroughs, S. Evans, A.



- Hamnett, A. F. Orchard, N. V. Richardson, *J. Chem. Soc. Faraday Trans. 2* **1974**, 70, 1895–1911; c) D. C. Crans, H. Chen, R. A. Felty, *J. Am. Chem. Soc.* **1992**, 114, 4543–4550.
- [2] a) P. B. Armentrout, *Ann. Rev. Phys. Chem.* **2001**, 52, 423–461; b) R. A. J. O'Hair, G. N. Khairallah, *J. Cluster. Sci.* **2004**, 15, 331–363; c) L. Operti, R. Rabezzana, *Mass. Spectrom. Rev.* **2006**, 25, 483–513; d) D. K. Böhme, H. Schwarz, *Angew. Chem. Int. Ed.* **2005**, 44, 2336–2354; e) G. A. Somorjai, A. M. Contreras, M. Montano, R. M. Rioux, *Proc. Natl. Acad. Sci. U.S.A.* **2006**, 103, 10577–10583; f) G. K. Koyanagi, D. Carai-man, V. Blagojevic, D. K. Bohme, *J. Phys. Chem. A* **2002**, 106, 4581–4590.
- [3] a) I. T. Horvath, *Encyclopedia of Catalysis*, Wiley International, **2003**; b) J. L. G. Fierro, *Metal Oxides*, Taylor & Francis Group, LLC, **2006**.
- [4] W. Plass, *Coord. Chem. Rev.* **2003**, 237, 205–212.
- [5] H. Ulrich (Ed.), *The Chemistry and Technology of Isocyanates*, Wiley, New York, **1996**.
- [6] D. Randall, S. Lee (Eds.), *The Polyurethanes Book*, John Wiley & Sons, New York, **2002**.
- [7] M. Schmeisser, *Angew. Chem.* **1955**, 67, 493.
- [8] B. A. Smart, H. E. Robertson, D. W. H. Rankin, E. G. Hope, C. J. Marsden, *J. Chem. Soc., Dalton Trans.* **1999**, 473–477.
- [9] D. Schröder, J. Loss, M. Engeser, H. Schwarz, H. C. Jankowiak, R. Berger, R. Thissen, O. Dutuit, J. Döbler, J. Sauer, *Inorg. Chem.* **2004**, 43, 1976–1985.
- [10] a) Q. Sun, Z. Li, X. Q. Zeng, W. G. Wang, Z. Sun, M. F. Ge, D. X. Wang, D. K. W. Mok, F. T. Chau, *ChemPhysChem* **2005**, 6, 2032–2035; b) Z. Sun, D. Wang, R. Ding, M. F. Ge, D. X. Wang, F. T. Chau, D. K. W. Mok, *J. Chem. Phys.* **2003**, 119, 293–299.
- [11] a) X. J. Zhu, M. F. Ge, J. Wang, Z. Sun, D. X. Wang, *Angew. Chem. Int. Ed.* **2000**, 39, 1940–1943; b) J. Wang, Z. Sun, X. Zhu, X. Yang, M. F. Ge, D. Wang, *Angew. Chem. Int. Ed.* **2001**, 40, 3055–3057; c) M. F. Ge, J. Wang, Z. Sun, X. Zhu, D. Wang, *J. Chem. Phys.* **2001**, 114, 3051–3054; d) X. Q. Zeng, F. Liu, Q. Sun, M. F. Ge, J. Zhang, X. Ai, L. Meng, S. Zheng, D. Wang, *Inorg. Chem.* **2004**, 43, 4799–4801.
- [12] W. G. Wang, M. F. Ge, L. Yao, X. Q. Zeng, Z. Sun, D. X. Wang, *ChemPhysChem* **2006**, 7, 1382–1387.
- [13] C. F. V. Mason, R. G. Behrens, *J. Less Common Met.* **1982**, 85, 21–26.
- [14] Y. Shechter, *Diabetes* **1990**, 39, 1–5.
- [15] J. Galy, R. Enjalbert, G. Jugie, J. Straehle, *J. Solid State Chem.* **1983**, 47, 143–150.
- [16] G. J. Christian, R. Stranger, B. F. Yates, *Inorg. Chem.* **2006**, 45, 6851–6859.
- [17] M. Alaei, P. Hofstra, C. Kirby, N. P. C. Westwood, *J. Chem. Soc., Dalton Trans.* **1990**, 1569–1573.
- [18] M. Fehér, M. J. Smit, T. Pasinszki, T. Veszprémi, *J. Phys. Chem.* **1995**, 99, 8604–8607.
- [19] B. Ruscic, J. Berkowitz, *J. Chem. Phys.* **1994**, 100, 4498–4508.
- [20] R. Prasad, *J. Chem. Phys.* **2004**, 120, 10089–10100.
- [21] L. Yao, X. Q. Zeng, M. F. Ge, W. G. Wang, Z. Sun, L. Du, D. X. Wang, *Eur. J. Inorg. Chem.* **2006**, 2469–2472.
- [22] M. J. Frisch, G. W. Trucks, H. B. Schlegel, G. E. Scuseria, M. A. Robb, J. R. Cheeseman, J. A. Montgomery Jr, T. Vreven, K. N. Kudin, J. C. Burant, J. M. Millam, S. S. Iyengar, J. Tomasi, V. Barone, B. Mennucci, M. Cossi, G. Scalmani, N. Rega, G. A. Petersson, H. Nakatsuji, M. Hada, M. Ehara, K. Toyota, R. Fukuda, J. Hasegawa, M. Ishida, T. Nakajima, Y. Honda, O. Kitao, H. Nakai, M. Klene, X. Li, J. E. Knox, H. P. Hratchian, J. B. Cross, C. Adamo, J. Jaramillo, R. Gomperts, R. E. Stratmann, O. Yazyev, A. J. Austin, R. Cammi, C. Pomelli, J. W. Ochterski, P. Y. Ayala, K. Morokuma, G. A. Voth, P. Salvador, J. J. Dannenberg, V. G. Zakrzewski, S. Dapprich, A. D. Daniels, M. C. Strain, Ö. Farkas, D. K. Malick, A. D. Rabuck, K. Raghavachari, J. B. Foresman, J. V. Ortiz, Q. Cui, A. G. Baboul, S. Clifford, J. Cioslowski, B. B. Stefanov, G. Liu, A. Liashenko, P. Piskorz, I. Komaromi, R. L. Martin, D. J. Fox, T. Keith, M. A. Al-Laham, C. Y. Peng, A. Nanayakkara, M. Challacombe, P. M. W. Gill, B. Johnson, W. Chen, M. W. Wong, C. Gonzalez, and J. A. Pople, *Gaussian 03 (Revision B.01)*, Gaussian, Inc., Pittsburgh PA, **2003**.
- [23] A. D. Becke, *J. Chem. Phys.* **1993**, 98, 5648–5652.
- [24] C. Lee, W. Yang, R. G. Parr, *Phys. Rev. B* **1988**, 37, 785–789.
- [25] W. V. Niessen, J. Schirmer, L. S. Cederbaum, *Comput. Phys. Rep.* **1984**, 1, 57–125.
- [26] T. Koopmans, *Physica* **1934**, 1, 104–113.

Received: October 25, 2007

Published Online: February 5, 2008